Reactivity of Alloxydim: Force and Reaction Electronic flux profiles

Juan J. Villaverde[a], Pilar Sandín-España[a], José L. Alonso-Prados[a], Manuel Alcamí[c,b,d] , Al Mokhtar Lamsabhi[b,c,*]

[a] *Plant Protection Products Unit, DTEVPF, INIA, Crta. La Coruña, Km. 7.5, 28040 Madrid, Spain*
[b] *Departamento de Química, Facultad de Ciencias, Módulo 13, Universidad Autónoma de Madrid, 28049 Madrid, Spain*
[c] *Institute for Advanced Research in Chemical Sciences (IAdChem), Universidad Autónoma de Madrid, 28049 Madrid, Spain*
[d] *Instituto Madrileño de Estudios Avanzados en Nanociencias (IMDEA-Nanociencia), 28049 Madrid, Spain*
Corresponding autor: mokhtar.lamsabhi@uam.es

Abstract:

The Reaction force profile and the electronic reaction flux concepts were explored for Alloxydim and some of its derivatives at B3LYP/6-311G(d,p) level of theory. The exploration was achieved by varying the dihedral angle located nearby the most reactive region. The main objective is to understand the response of the oxime group against this perturbation together with highlighting the intrinsic structural and the electronic reorganization. The results show that the rotation of the dihedral angle triggers the alloxydim to go through three transition states. The first step of the transformation begins by the rupture of the hydrogen bond and is characterized by a pronounced structural reorganization. To return to the same structure in the last step of the process the electronic reorganization are more important. In between, N-O bond goes through different state of the reinforcement and weakening showing the ideal conformer where the oxime fragment might be dissociated.

Keywords: Pesticides, Reaction force profile, Reaction Electronic flux, conceptual DFT,

Introduction:

National and International authorities as well as environmental agencies worldwide have promoted legislations to the protection of public health and environment. Among different things, they demand a rational use of pesticides, the reduction in the level of pesticide residues in food and in the environment and the knowledge whether they are safe. In this sense, the European Union (EU) has one of the most developed pesticide legislation. Since the adoption of the Council Directive 91/414/EEC, which was later replaced by the current Regulation (EC) No. 1107/2009, any pesticide must past a rigorous assessment process that proves that it does not pose risk before marketed in any Member State of the EU.[1] Public institutions, such as INIA in Spain, ANSES in France, etc., collaborate with the European Food Safety Authority (EFSA) to perform this evaluation. However, the process entails a large number of experimental studies, which in many cases involves a high cost and delay overtime. This fact affects the competitiveness of the community agriculture by delaying the incorporation of the latest advances in the sector. Taking into account that Regulation (EC) No. 1107/2009 states that authorization of pesticides should be performed based on current scientific and technical knowledge, an alternative approach could take advantage of computational chemistry to accelerate the process.[2]

To understand the reactivity of pesticides and their physicochemical properties is key to predict their harmful effect on human and animal health and on the environment. Therefore, the study these issues by *ab initio* or Density functional theory methods might be an easy and costless task. Recently, we started different studies on an herbicide alloxydim known by its pronounced toxicity and the damage that it photodegradation could cause in the environment (see scheme).[3,4] Our first attempts were to figure out the most stable conformer and the capability of the oxime fragment dissociation.[5,6] In fact, it is thought that the toxicity of this compound is ligated to its ability to detach this group which was the reason why we decided to dedicate our second study on the products of the oxime rupture.[5] In this case we reported the resulting molecules commonly called degradation products (DPs) from the viewpoints of their homoloytic and heterolytic departures.

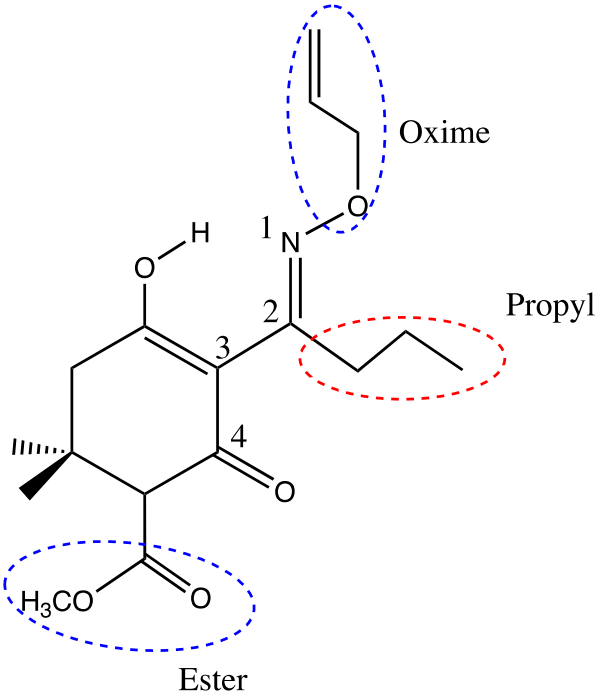

The mechanism of oxime intoxication is thought to lie in its interaction with nerve agents.[7] To deactivate it, many oxime-based drugs have been approved that are based on the spatial orientation of the oxime group.[8] So, it is essential to know the orientation of the active group to determine its toxicity as poisoning or as a drug. The side chain substituents at position 2 (see scheme) in alloxydym derivatives show great influence in the herbicidal activity and so in its toxicity.[4] Substituents other than *n*-Pr, i.e. H and Ph, brought about no or very low effectiveness. These results are comparable to the rotational energy barrier for benzidine (0 to 2.61 kcal/mol).[9] This rotational freedom allows benzidine and their selected derivatives to freely interact with various components in real life systems and is thus the possible reason for their toxicity.

In the present study we focused on the perturbation of the most reactive region. Avoiding the rupture of the oxime our main objective is to follow up the electronic and the structure variations when the dihedral angle that contain this group (marked in the scheme) is changed. To get more insights on this perturbation we decided to analyze the effect of the propyl group substitution by hydrogen, phenyl and chlorine group.

The theoretical Framework:

The intrinsic chemical change following a variation of one of the internal coordinate of a chemical entity can be understood in terms of geometrical changes and the reordering of the electron densities involved in the process.[8] Therefore, identifying structural and electronic changes taking place along the coordinate variation produces valuable information on the molecule transformation and can be analyzed by the reaction force concept.[10] In fact, following the energy variation along the dihedral angle evolution could shed light on the different saddle points that encompass the reactivity of the systems under study. Starting from the structure with the lowest energy value associated to a given dihedral angle we can construct the energy profile, (E(θ)), of the system that links the transition state to the reactants and products, in our case the energy minima structures "conformers". The reaction force is defined as the derivative of E(θ) with respect to angle variation θ by the expression,[11]

$$F(\theta) = -\frac{dE(\theta)}{d\theta} \qquad (1)$$

For any elementary step of a chemical changes, the reaction force is characterized by a minimum and a maximum located at ξ_1 and ξ_2 which delimitate three regions along the coordinate: the first one associated with the reactants ($\theta_R \leq \theta \leq \theta_1$) in which the reactants are prepared for the reaction mainly through structural reordering. The second one ($\theta_1 \leq \theta \leq \theta_2$) is the transition state region, corresponds to the region where most electronic changes due to bond formation and breaking take place. Finally, the third region, ($\theta_2 \leq \theta \leq \theta_P$), is associated with structural relaxation to reach the products of the reaction.[12] This well delimited reaction regions help to locate all the chemical events that take place in a reaction coordinates, thus giving a detailed picture of the system transformation. The activation energy and the energy necessary to attain the minima can also be obtained through the analysis of reaction force profile in the following decomposition in terms of reaction works.

$$\Delta E^{\neq} = W_1 + W_2 \qquad (2)$$

where,

$$W_1 = -\int_{\theta_R}^{\theta_1} F(\theta)d\theta \quad \text{and} \quad W_2 = -\int_{\theta_1}^{\theta_{TS}} F(\theta)d\theta \quad (3)$$

W_1 stands for the structural reorganizations to get the transition state from the reactant while *W_2* encompass the major electronic variations in the transition state region.

To deeply understand the changes along the dihedral variation the conceptual DFT has been checked.[13,14] This derivate theory from DFT offers an extended range of theoretical tools that can allow to study and understand the electronic changes which are directly associated to physicochemical properties of molecular systems. The electronic chemical potential, μ, for a system of N electrons indicates the escaping tendency of electrons from sites of high chemical potential to low chemical potential and associated to the negative of electronegativity, χ.[15] It is defined as the derivative of the total energy with respect to N when the external potential, *v(r)*, remains constant.

$$\mu(r) = \left(\frac{\partial E(r)}{\partial N}\right)_{v(r)} = -\chi \qquad (4)$$

The reaction electronic flux[16], J(θ), associated to a chemical transformation can be defined using equation 5:

$$J(\theta) = -\frac{d\mu(\theta)}{d\theta} \quad (5)$$

The interpretation of the reaction electronic flux results from the analogy with classical thermodynamics. Positive values of J(θ) should be associated to spontaneous rearrangements of the electron density driven by bond strengthening or forming processes; negative values of J(θ) are indicating nonspontaneous rearrangements of the electron density that are mainly driven by bond weakening or breaking processes.[16]

Computational Details:

The optimization of the stationary points of structures under study was achieved at B3LYP/6-311G(d,p) level of theory.[17,18] The rotation of the concerned fragment has been followed by a relaxed scan at the same level of theory by means of

Gaussian 16 series of programs.[19] The electronic population analysis was done by the quantum theory of atoms in molecule theory (QTAIM), by using the AIMAll program.[20]

Results & Discussions:

Our purpose as mentioned above is to highlight the electronic changes in alloxydim on the most reactive site. To get deeper on these variations we substitute the propyl of alloxydim by different substituents to try to recover many aspects. For this end, as can be shown in scheme 2, propyl was replaced by hydrogen, aryl or chlorine. To follow up the electronic and the structural changes of these derivates along the dihedral variation we constructed the energy profile starting from the most stable structure.[5] This means that the exploration of the energy variation begins at $\theta_{C1,C2,C3,N} \approx -180^{o}$ and finishes at $\theta_{C1,C2,C3,N} \approx 220^{o}$. The choice of this structure comes of our recent exploration of the different isomers of the alloxydim.[5] In figure 1 are represented the energy profile of the four compounds under study. The first conspicuous conclusion from this figure is that the rotation of the angle $\theta_{C1,C2,C3,N}$ is energetically more demanding in aloxydim compared to the other species. Even with the electronic repulsion that can be presented by the aryl derivate alloxydim needs to overpass approximately more than 80 kJ/mol between the two minima while for the phenyl substitution this quantity does not exceed 54 kJ/mol. In the case of chlorine substitution this value is about 33 kJ/mol. This is a simple image of the variation of the energy within the increase of the dihedral angle. However, if we explore the reaction force profile (see figure 2) we would be able to reach more valuable information. In fact, the reaction force profile as presented in figure 2 shows that the rotation process of the dihedral angle, θ, triggers alloxydim and its derivatives to go through three different maxima, called, TS1, TS2 and TS3. The minima between them are hidden due to the highest energy barriers obtained. Yet, the maxima have their origin on the middle point between two inflections of the reaction force curve which delimitate three regions of the compound transformation. Each one of these regions, as has been defined by Toro-labbé,[10] can show the structural and the electronic reorganizations in each step of the systems under study. To quantify these transformations Toro-Labbé et al.

proposed to calculate the works W_1 and W_2 and their participation in the activation energy, as defined above.[16]

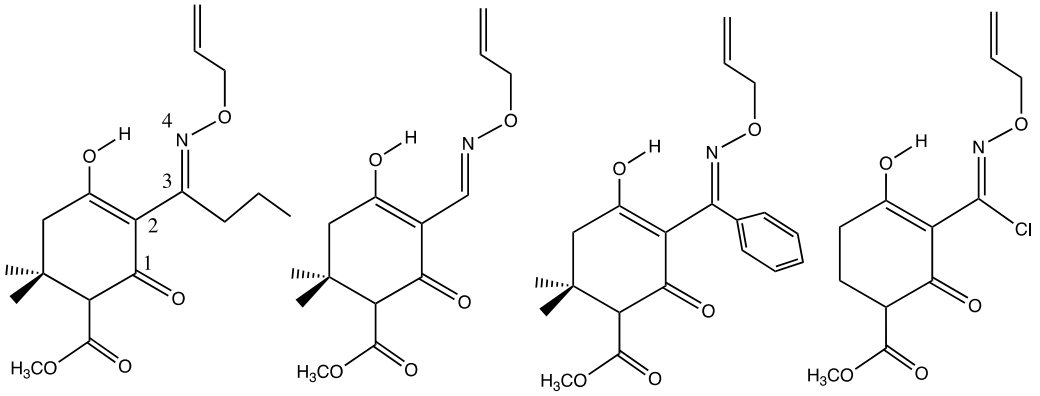

Scheme 2: The structure of the different derivatives of Alloxydim under study.

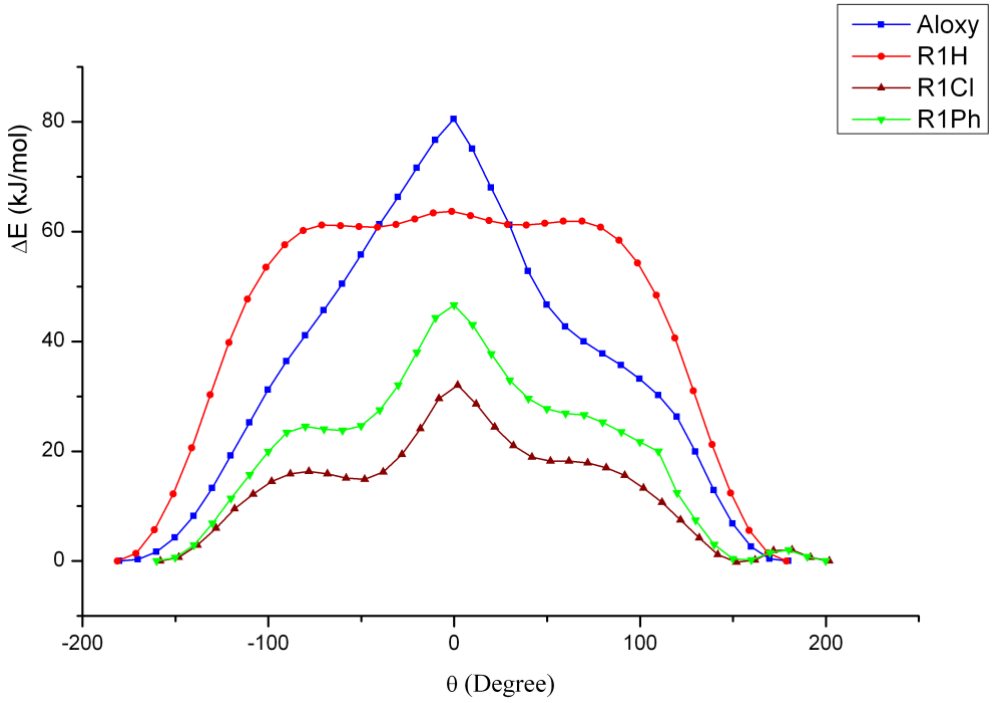

Figure 1: Energy profile of alloxydim and its derivatives along the variation of the dihedral angle θ.

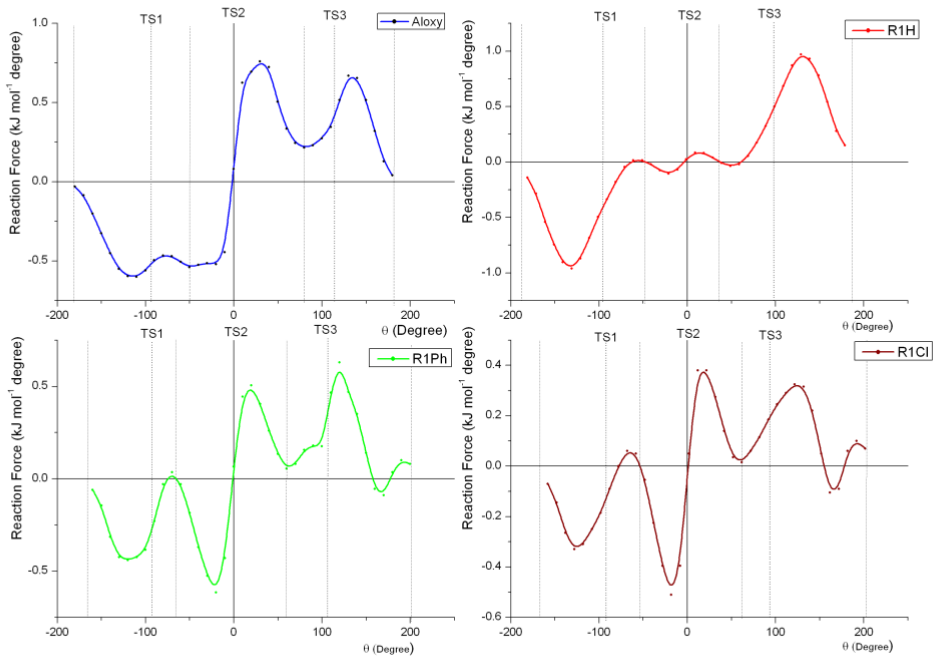

Figure 2: The reaction force profile of alloxydim and its derivatives along the rotation.

For alloxydim and its derivatives the rotation of the dihedral angle θ, shows that the system goes through three steps. The first one is associated to the rupture of the hydrogen bond in the most stable conformers and is shown the highest barrier energy along the process. Based on the works values W1 and W2 deduced from figure 2 and listed in table 1, the highest activation energy is reported for R1=H derivative. The structural rearrangement is about 53 % of the activation energy whereas the electronic reorganization is about 47%. The alloxydim on the other hand presents more structural than electronic reorganization with values about -19.2 and 17.1 kJ/mol, respectively. This can be explained by the size of the isopropyl of alloxydim which needs more structural accommodation than the hydrogen as substituent. In the same step with respect to the phenyl substituent, the structural and the electronic rearrangements to gain the first transition state, TS_1, are similar because probably of the π cloud of the aromatic substituent (see table 1).

Table 1: Works W_1 and W_2 performed by the system along the rotation of angle θ at each step of the process. $\Delta E^{\#}$ the energy barrier associated to each step.

	TS_1			TS_2			TS_3		
	W_1	W_2	$\Delta E^{\#}$	W_1	W_2	$\Delta E^{\#}$	W_1	W_2	$\Delta E^{\#}$
Aloxy	-19.2	-17.1	-36.3	-15.7	-6.7	-22.3	0	12.2	12.2
R1=H	-30.3	-26.9	-57.2	-1.4	-1.1	-2.5	-0.5	7.95	7.5
R1=Ph	-11.4	-11.4	-22.8	-14	-7.1	-21.1	0	8.5	8.5
R1=Cl	-6.1	-9.6	-15.7	-9.1	-6.2	-15.3	0	2.8	2.8

Following the rotation of the dihedral angle the second step appears energetically less demanding than the first one. The highest barrier is observed for alloxydim and its phenyl derivate (R1=Ph). In all the cases the structural reorganization is the most dominant one. This is expected because this step represents a typical rotational transition state where the substituents moved by the angle should adapt their structure to fit with the new structural form of the molecule. It is worth noting that the lowest barrier is observed for R1=H, about -2.5 kJ/mol accordingly with the size of the substituent which does not required nor elevated structural nor electronic changes to overpass the transition state. In what concerns the last step of the energy profile, nearby TS_3, it is clear that structural movements are practically null in all the cases. The electronic rearrangement is the most dominant instead. This can be understood by the necessity of the system under study to attain again the hydrogen bond arrangement which basically needs an electronic adaptation of the molecule.

The balance between the structural and the electronic changes along the angle variation in the energy profile can be viewed also by analyzing the reaction electronic flux profile. In fact, in the first step of the rotation of all the systems under scrutiny we can observe a positive value of $J(\theta)$ which is an indication of a bond strengthening and spontaneous processes. The evolution of the system in this step from the rupture of the hydrogen bond, OH--N, at $\theta \approx -180^{o}$ leaves place to reinforcement of the associated bonds and the apparition of new weak hydrogen

bonds. This can be ratified by analyzing different structures in some critical points of the energy profile by using the QTAIM population analysis. Indeed at the angle θ =-160 we observe, for alloxydim, a hydrogen bond provided by the hydroxyl group with an electronic density at the bond critical point (BCP) about 0.058 a.u.. When moving to θ=-90, the density at this BCP decreases to attain approximately 0.017 a.u. which is accompanied by the appearance of small H--H bonds (see figure 4a) which are basically provided by the CH groups. The oxime group along the rotation is affected by the structural and the electronic reorganization. In fact, while N--O bond along θ variation is enfeebled the nearby bonds in 6-membered ring become reinforced. This might be an indication that the rupture of this group may occur during the conformational transformation.

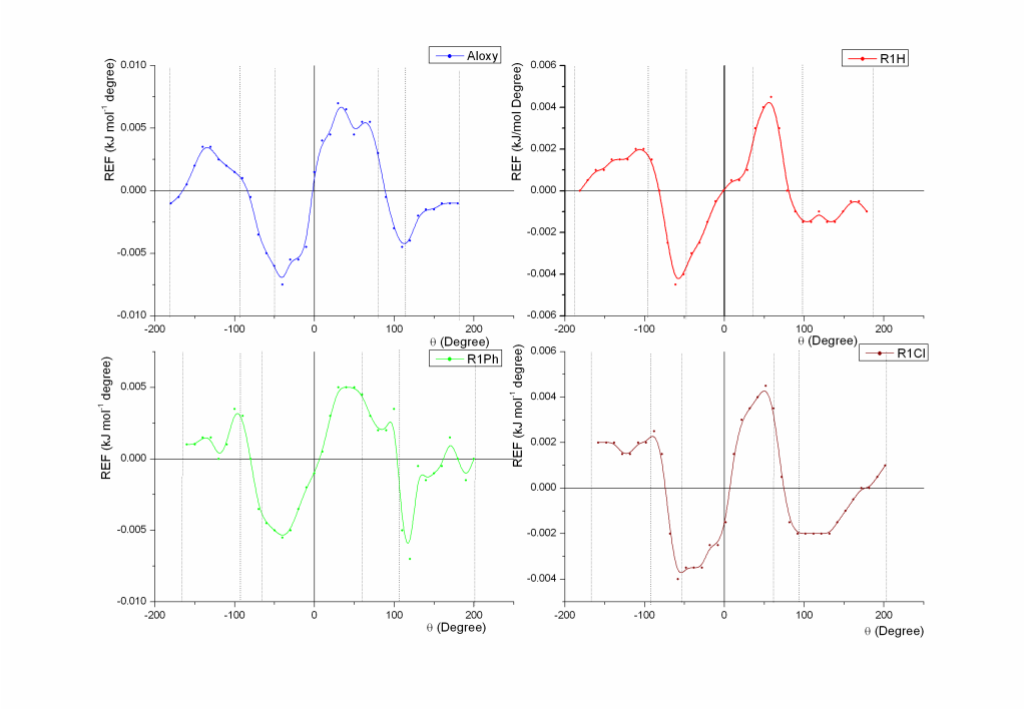

Figure 3: Reaction electronic flux profile of the different substituents along the variation of the angle θ.

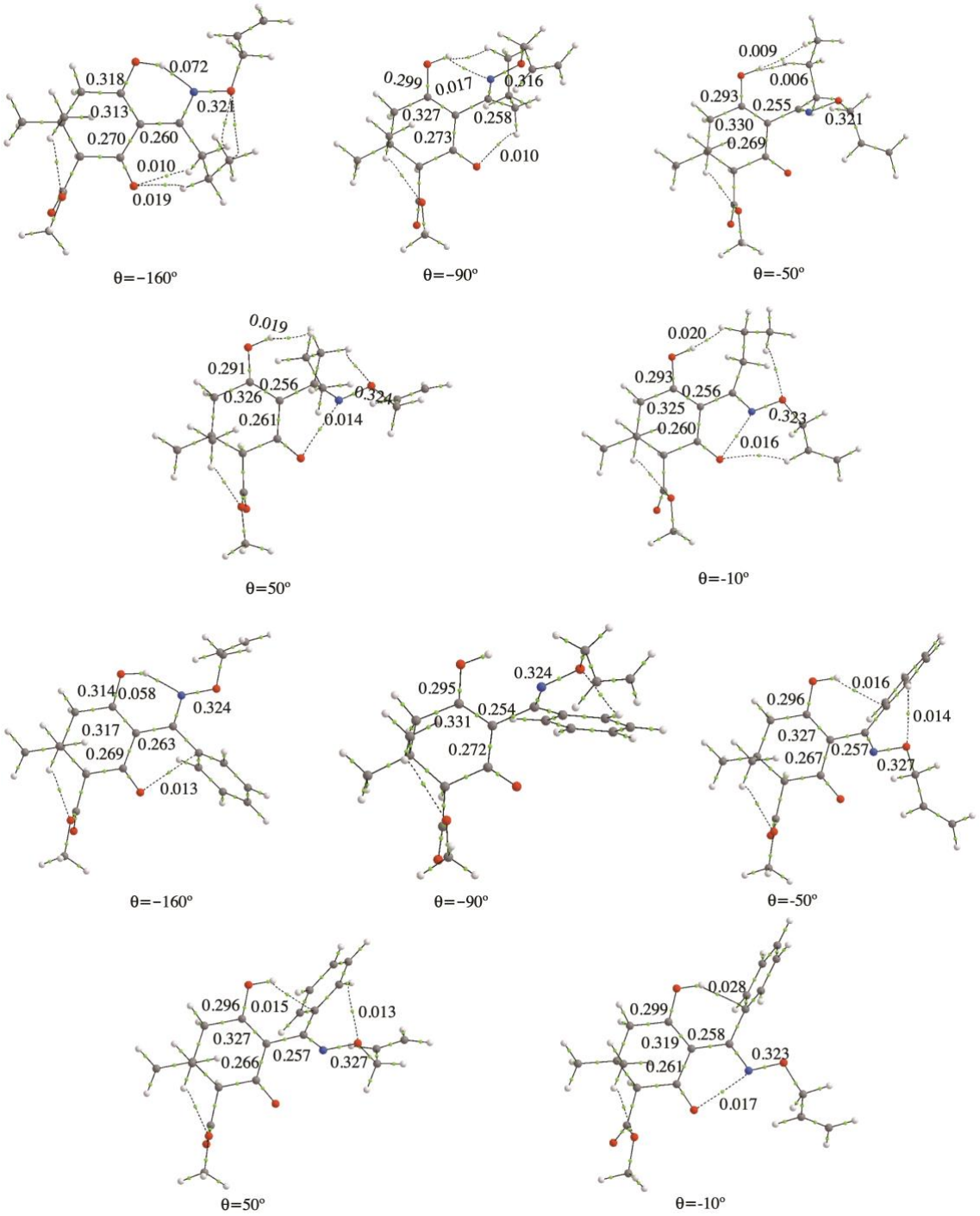

Figure 4: The QTAIM analysis of some critical points along the θ variation in the case of Alloxydim(a) and its phenyl derivative (R1=Ph). The values at the BCP are in a.u.

The REF profile presents negative values when the system overcomes the first transition state. This indicates that the molecule resumes the reinforcement of the electronic density on the bonds nearby the rotation. Form the QTAIM analysis, N—O bond is reinforced while some bonds of the six membered ring are enfeebled. In fact, the electron density at the BCP of N--O goes from 0.316 u.a. in θ=-90º to 0.321 a.u. in θ=-50º. It is to note that between the alloxydim and its phenyl counterpart the small interaction between the

different group that are stabilizing the system along the rotation are OH--HC bonds for the former whereas for the later are HB provided carbon atom of the ring as acceptor.

Conclusions:

The intrinsic rotation of the dihedral angle θ of alloxydim and its derivatives shows that the system goes through three steps. The energy barrier in each step involves different electrostatic interactions that stabilize the molecule. In alloxydim these interactions are provided by the CH of isopropyl group favoring dehydrogen interaction while for its phenyl derivative we found small HB bonds involving a carbon atom of the aryl group. The analysis of the force profile shows that the major structural reorganizations are done in the first and the second steps of the rotation process. In the last step the electronic reorganization is the dominant one. The N-O bond is weakened when moving the dihedral angle which might indicates that the oxime group could be dissociated along the conformational transformation.

Acknowledgments:

We acknowledge the financial support from PID2019-110091GB-I00 (MICINN) of the Ministerio de Ciencia, Innovación y Universidades of Spain and the PRIES-CM project Ref: Y2020/EMT-6290 from the Comunidad Autónoma de Madrid. The authors would also like to thank the *Centro de Computación Científica* of the UAM (CCC-UAM) for the generous allocation of computer time and for their continued technical support.

References:

1 E. Union, Regulation (EC) No 1107/2009, in *Off J Eur Union L*, 2009, vol. 309, pp. 1.
2 J. J. Villaverde, C. López-Goti, M. Alcamí, A. M. lamsabhi, J. L. Alonso-Prados and P. Sandín-España, *Pest Management Science*, 2017, **73**, 2199.
3 P. Sandín-España, B. Sevilla-Morán, L. Calvo, M. Mateo-Miranda and J. L. Alonso-Prados, *Microchemical Journal*, 2013, **106**, 212.
4 J. J. Villaverde, I. Santín-Montanyá, B. Sevilla-Morán, J. L. Alonso-Prados and P. Sandín-España, *Molecules*, 2018, **23**, 993.
5 J. J. Villaverde, P. Sandín-España, J. L. Alonso-Prados, A. M. lamsabhi and M. Alcamí, *The Journal of Physical Chemistry A*, 2018, **122**, 3909.
6 J. J. Villaverde, P. Sandín-España, J. L. Alonso-Prados, A. M. lamsabhi and M. Alcamí, *Computational and Theoretical Chemistry*, 2018, **1143**, 9.
7 J. Dhuguru, E. Zviagin and R. Skouta, *Pharmaceuticals*, 2022, **15**, 66.
8 U. Sarkar, D. R. Roy, P. K. Chattaraj, R. Parthasarathi, J. Padmanabhan and V. Subramanian, *Journal of Chemical Sciences*, 2005, **117**, 599.
9 J. C. Coburn, P. D. Soper and B. C. Auman, *Macromolecules*, 1995, **28**, 3253.

10 A. Toro-Labbé, *The Journal of Physical Chemistry A*, 1999, **103**, 4398.
11 J. Martinez and A. Toro-Labbé, *Journal of Mathematical Chemistry*, 2009, **45**, 911.
12 B. Herrera and A. Toro-Labbé, *Chemical Physics Letters*, 2001, **344**, 193.
13 P. Geerlings, *Pharmaceuticals*, 2022, **15**, 1112.
14 P. Geerlings, F. De Proft and W. Langenaeker, *Chemical Reviews*, 2003, **103**, 1793.
15 R. G. Parr and W. Yang, *Density Functional Theory of Atoms and Molecules*, Oxford University Press, New York, 1989.
16 E. Echegaray and A. Toro-Labbé, *The Journal of Physical Chemistry A*, 2008, **112**, 11801.
17 A. D. Becke, *J. Chem. Phys.*, 1993, **98**, 5648.
18 C. T. Lee, W. T. Yang and R. G. Parr, *Phys. Rev. B*, 1988, **37**, 785.
19 M. J. Frisch, G. W. Trucks, H. B. Schlegel, G. E. Scuseria, H. Frisch, M. J. Trucks, G. W. Schlegel, H. B. Scuseria, G. E. Robb, M. A. Cheeseman, J. R. Scalmani, G. Barone, V. Mennucci, B. Petersson, G. A. Nakatsuji, H. Caricato, M. Li, X. Hratchian, H. P. Izmaylov, A. F. Bloino, J. Zheng, G. Sonnenberg, J. L. Hada, M. Ehara, M. Toyota, K. Fukuda, R. Hasegawa, J. Ishida, M. Nakajima, T. Honda, Y. Kitao, O. Nakai, H. Vreven, T. J. Montgomery, J. A. Peralta, J. E. Ogliaro, F. Bearpark, M. Heyd, J. J. Brothers, E. Kudin, K. N. Staroverov, V. N. Kobayashi, R. Normand, J. Raghavachari, K. Rendell, A. Burant, J. C. Iyengar, S. S. Tomasi, J. Cossi, M. Rega, N. Millam, J. M. Klene, M. Knox, J. E. Cross, J. B. Bakken, V. Adamo, C. Jaramillo, J. Gomperts, R. Stratmann, R. E. Yazyev, O. Austin, A. J. Cammi, R. Pomelli, C. Ochterski, J. W. Martin, R. L. Morokuma, K. Zakrzewski, V. G. Voth, G. A. Salvador, P. Dannenberg, J. J. Dapprich, S. Daniels, A. D. Farkas, Ö. Foresman, J. B. Ortiz, J. V. Cioslowski and J. Fox, Gaussian 09, Gaussian Inc,, Wallingford, CT, Revision E01 edn., 2017.
20 T. A. Keith, AIMAll http://aim.tkgristmill.com, Overland Park, 17.11.14 edn., 2018.